

# Rectenna Design Optimized by Binary Genetic Algorithm for Hybrid Energy Harvesting Applications Across 5G Sub-6 GHz Band

Ahmed Rifaat Hamad<sup>1</sup>, Ammar Al-Adhami<sup>2</sup>, Nouf Abd Elmunim<sup>3\*</sup>, Mohammad Alibakhshikenari<sup>4\*</sup>, Bal Virdee<sup>5</sup>, Hasan Salman Hamad<sup>6</sup>, Renu Jayanthi<sup>5</sup>, Dion Mariyanayagam<sup>5</sup>, Innocent Lubangakene<sup>5</sup>, Sunil Kumar<sup>5</sup>, Salahuddin Khan<sup>7</sup>, Yi Tang<sup>8</sup>, Lida Kouhalvandi<sup>9</sup>, Taha A. Elwi<sup>10\*</sup>, Mohsin Ali Ahmed<sup>11</sup>, and Nasr Rashid<sup>12, 13</sup>

<sup>1</sup>Electric Department, Institution of Technology, Middle Technical University, Baghdad, Iraq; [iatrcbaghdad@gmail.com](mailto:iatrcbaghdad@gmail.com)

<sup>2</sup>Electronic Computer Center, Al-Karkh University of Science; [ammarisajjm@kus.edu.iq](mailto:ammarisajjm@kus.edu.iq)

<sup>3</sup>Department of Electrical Engineering, College of Engineering, Princess Nourah bint Abdulrahman University, P.O. Box 84428, Riyadh 11671, Saudi Arabia; [naasmal@pnu.edu.sa](mailto:naasmal@pnu.edu.sa)

<sup>4</sup>Electronics Engineering Department, University of Rome "Tor Vergata", 00133 Rome, Italy; [alibakhshikenari@ing.uniroma2.it](mailto:alibakhshikenari@ing.uniroma2.it)

<sup>5</sup>Center for Communications Technology, London Metropolitan University, London N7 8DB, United Kingdom; [b.virdee@londonmet.ac.uk](mailto:b.virdee@londonmet.ac.uk), [r.rajagurujayanthi1@londonmet.ac.uk](mailto:r.rajagurujayanthi1@londonmet.ac.uk), [d.mariyanayagam@londonmet.ac.uk](mailto:d.mariyanayagam@londonmet.ac.uk), [i.lubangakene1@londonmet.ac.uk](mailto:i.lubangakene1@londonmet.ac.uk), [s.kumar@londonmet.ac.uk](mailto:s.kumar@londonmet.ac.uk)

<sup>6</sup>Technical College of Engineering, Al-Bayan University, Baghdad, Iraq; [hasanss@albayan.edu.iq](mailto:hasanss@albayan.edu.iq)

<sup>7</sup>Sustainable Energy Technologies Center, College of Engineering, King Saud University, P.O.Box 800, Riyadh 11421, Saudi Arabia; [drskhan@ksu.edu.sa](mailto:drskhan@ksu.edu.sa)

<sup>8</sup>School of Electromechanical and Automotive Engineering, Yantai University, Yantai, 264005, China; [tangyi0319@126.com](mailto:tangyi0319@126.com)

<sup>9</sup>Department of Electrical and Electronics Engineering, Dogus University, Istanbul 34775, Turkey; [lida.kouhalvandi@ieee.org](mailto:lida.kouhalvandi@ieee.org)

<sup>10</sup>Islamic University Centre for Scientific Research, The Islamic University, Najaf, Iraq; [taelwi82@gmail.com](mailto:taelwi82@gmail.com)

<sup>11</sup>International Applied and Theoretical Research Center (IATRC), Baghdad Quarter, Iraq; [maahmed54646@gmail.com](mailto:maahmed54646@gmail.com)

<sup>12</sup>Electrical Engineering Department, College of Engineering, Jouf University, Sakaka, Aljouf 72388, Saudi Arabia

<sup>13</sup>Department of Electrical Engineering, Faculty of Engineering, Al-Azhar University, Nasr City, Cairo 11884, Egypt; [nasrrashid34.el@azhar.edu.eg](mailto:nasrrashid34.el@azhar.edu.eg)

\*Corresponding Authors: Nouf Abd Elmunim, Mohammad Alibakhshikenari, and Taha A. Elwi

**Abstract:** This paper presents a novel rectenna design for hybrid energy harvesting, optimized using a binary genetic algorithm (BGA) with binary coding to improve geometry, impedance matching, and radiation efficiency. The fabricated rectenna achieves reflection coefficients below -40 dB at 2.45 GHz and 5.8 GHz, demonstrating excellent impedance matching. A commercial rectifier (Powercast P21XXCSR-EVB), employing a voltage doubler topology and Schottky diodes (Skyworks SMS7630 and Avago HSMS 285B), is integrated for RF-to-DC conversion. Peak efficiencies of 90% at 2.45 GHz and 52% at 5.8 GHz are recorded at 11 dBm input power, while efficiencies above 80% and 50%, respectively, are maintained at 0 dBm. The rectifier also exhibits wide impedance bandwidths, with reflection coefficients of -23 dB and -18 dB at the respective frequencies. Outdoor testing yields DC output voltages of 92.6 mV (2.45 GHz) and 64 mV (5.8 GHz). The system's efficiency and adaptability under variable conditions make it ideal for low-power applications such as wireless sensor networks, IoT devices, and remote monitoring. Its robust performance across environments highlights its potential for autonomous energy harvesting in 5G and sub-6 GHz networks.

**Keywords:** Rectenna design, binary coding, energy harvesting, binary genetic algorithm (BGA), artificial intelligence (AI), 5G and sub-6GHz.

## I. Introduction

In the past decade, RF energy harvesting systems have gained significant attention due to their potential to provide self-sustaining power for low-energy devices such as wireless sensor networks (WSNs), Internet of Things (IoT) applications, and remote monitoring systems. Several designs have been proposed in the literature and are typically categorized into single-band, multi-band, and broadband rectennas. These systems employ a variety of rectenna and rectifier structures to enhance gain and energy conversion efficiency, with impedance matching circuits used to link rectifiers to rectennas for optimal performance.

Among notable developments, a voltage doubler rectifier with an open stub matching network and radial stub was proposed, achieving over 75% conversion efficiency at 20 dBm input power while suppressing higher-order harmonics using a triangular slot in the ground plane [1]. Another study introduced a compact L-probe patch rectenna with a dual-port stacked configuration that delivered efficiencies greater than 40%, producing more than 600 mV DC output under power densities exceeding  $500 \mu\text{W}/\text{m}^2$  [2].

Multi-band rectennas have also demonstrated promising results. For example, a slot rectenna with a triple-band rectifier operating at 2 GHz, 2.5 GHz, and 3.5 GHz used Inter-Digital Capacitors (IDCs) instead of lumped components to achieve peak conversion efficiencies of 53%, 31%, and 15.56%, respectively [3]. Similarly, a triple-band rectenna optimized for 0.85 GHz, 1.77 GHz, and 2.07 GHz showed high efficiency using a customized triple-band matching network [4].

Additional improvements have been made through broadband and multiport rectifier designs. A 16-port rectenna array connected to a triple-band rectifier achieved more than 40% RF-to-DC conversion efficiency, delivering  $7.3 \mu\text{W}$  in indoor and  $80 \mu\text{W}$  in outdoor environments [5]. Another design featuring three parallel rectifier branches operating at 0.9 GHz, 1.8 GHz, and 2.45 GHz maintained conversion efficiencies above 46.5% for all bands at 0 dBm input power [6].

A microstrip line-fed open-loop hexagonal rectenna with a partial ground plane was introduced for triple-band operation, supporting dual polarization and wide impedance bandwidths for GPS, LTE, and satellite communication bands [7]. Additionally, a quad-band multiport RF harvester capable of collecting ambient RF energy from GSM-900, GSM-1800, 3G, and Wi-Fi bands achieved rectification efficiencies up to 66.52%, outperforming many earlier multi-band designs [8].

Despite these advancements, several limitations persist in current rectenna technologies:

- Efficiency tends to degrade at higher frequencies.
- Multi-band rectifier architectures often introduce greater design complexity, making fabrication more challenging.
- Many designs rely exclusively on RF energy harvesting, which may be insufficient for continuous operation in low-power ambient environments.
- Some systems achieve high efficiency only at elevated input power levels (often above 10 dBm), reducing effectiveness in scenarios with limited available RF power.

These limitations are summarized in Table 1, which provides a comparative overview of prior rectenna designs in terms of development focus, key advantages, and existing challenges. This table highlights the trade-offs encountered in previous work

and underscores the need for a more robust, dual-band, and AI-optimized approach to energy harvesting.

Table 1: Summary of previous rectenna designs and their key features.

Ref.	Development	Advantages	Limitations
[1]	Uses a voltage doubler rectifier with an open stub matching network and a radial stub for impedance matching.	Achieves high conversion efficiency (~75%) at 20 dBm input power while suppressing second and third-order harmonics.	Requires high input power to maintain efficiency, making it less effective in low-power environments.
[2]	Employs a dual-port rectenna consisting of stacked single-port patch rectennas.	Achieves >40% efficiency and generates >600 mV DC output for power densities exceeding 500 $\mu\text{W}/\text{m}^2$ .	The stacked structure increases complexity and fabrication costs, limiting its practical deployment.
[3]	Introduced a triple-band rectifier at 2 GHz, 2.5 GHz, and 3.5 GHz, replacing lumped components with Inter-Digital Capacitors (IDCs).	Achieves maximum efficiencies of 53%, 31%, and 15.56% at respective frequencies, improving performance.	The efficiency drops significantly at higher frequencies, and fabrication complexity increases.
[4]	Operates at 0.85 GHz, 1.77 GHz, and 2.07 GHz, using a customized matching network for improved efficiency.	Demonstrates high efficiency across multiple frequency bands, making it suitable for multi-band energy harvesting.	Design complexity increases, making integration into compact circuits challenging.
[5]	Uses a 16-port rectenna array connected to a triple-band rectifier to enhance energy capture.	Achieves >40% RF-to-DC conversion efficiency and provides 7.3 $\mu\text{W}$ (indoor) and 80 $\mu\text{W}$ (outdoor) output power.	The system is bulky, limiting its use in miniaturized, portable applications.
[6]	Designed a triple-band rectifier with three parallel branches operating at 0.9 GHz, 1.8 GHz, and 2.45 GHz.	Maintains above 46.5% efficiency for all bands under 0 dBm input power, improving low-power performance.	The design complexity and power management challenges hinder practical implementation.
[7]	Introduced a hexagonal patch rectenna with a partial ground plane for triple-band operation.	Provides dual polarization and wide impedance bandwidths (14.7%, 6.8%, and 13.1%) at GPS, LTE, and satellite bands.	The rectenna design requires precise tuning, making fabrication and repeatability a concern.
[8]	Designed to scavenge ambient RF energy from GSM-900, GSM-1800, 3G, and Wi-Fi bands.	Achieves high rectification efficiency (~66.52%), outperforming many earlier designs.	The system is limited to existing ambient RF bands, restricting adaptability to newer wireless technologies.
[9]	Uses a Texas Instruments eZ430-RF2500 sensor operating at LTE 700, GSM 850, and ISM 900 bands.	Provides up to 45% efficiency across multiple bands, improving applicability for IoT.	The power harvested is low, making it unsuitable for high-power applications.
[10]	Applied AI and GA to optimize rectenna parameters and structures.	Enables real-time design optimization, enhances gain, bandwidth, and RF-to-DC conversion efficiency.	Computationally intensive, requiring high processing power and longer optimization time.
[11]	Broadband CP rectenna with AMC on FR4 substrate.	AR bandwidth of 19.6%, PCE ~65% at 7 dBm, effective in low input power range.	AMC increases structural complexity and size.
[12]	Traveling-wave antenna array rectenna at 12 GHz.	Wide angular coverage (-65° to 65°), PCE ~45% at 2.86 mW/cm <sup>2</sup> .	Complexity in array and combiner circuits.
[13]	Flat-panel rectenna with dual-voltage rectifier at 5.8 GHz.	Coverage angle of ~144.6°, peak RF-to-DC conversion efficiency of 51.8%.	Limited to single-band operation.
[14]	Hybrid RF-solar harvester with bowtie periodic antenna surface.	Integrates solar and RF sources, improved overall efficiency.	Complexity in spatial configuration and electrical integration.
[15]	Compact stacked multisector rectenna array at 5.9 GHz.	Near-isotropic coverage, hybrid dc combining, enhanced PCE across wide load range.	Complex multisector structure, increased fabrication complexity.

To address these challenges, artificial intelligence (AI) and optimization algorithms have been increasingly employed to enhance rectenna design and performance. AI-driven approaches such as Genetic Algorithms (GAs), Particle Swarm Optimization (PSO), and neural networks have shown strong potential in optimizing rectenna geometry, improving impedance matching, and maximizing rectifier efficiency. For instance, GA-based designs have led to notable gains in efficiency, bandwidth, and miniaturization [4]. Similarly, machine learning models have been applied to predict and fine-tune design parameters, minimizing reliance on computationally expensive simulations and enabling real-time adaptive optimization [16].

However, many of these AI-based methods have focused primarily on single-band or narrowband applications, leaving an opportunity for exploration in the realm of hybrid multi-band energy harvesting systems.

This study builds upon prior work in AI-driven rectenna design by implementing a Binary Genetic Algorithm (BGA) to optimize both the rectenna and rectifier design for hybrid energy harvesting. Unlike conventional GA methods, BGA applies structured binary coding to efficiently explore rectenna topologies, improving impedance matching and enabling wider operational bandwidths. Furthermore, this work focuses on simultaneous energy harvesting at 2.45 GHz and 5.8 GHz, optimizing both frequency bands through AI-guided tuning. The resulting system offers a highly efficient and scalable solution suitable for next-generation applications, including IoT and 5G networks.

Key points of this study are as follows:

- Artificial intelligence is employed in rectenna design for hybrid energy harvesting.
- A dual-band rectifier (2.45 GHz and 5.8 GHz) with voltage doubler topology and Schottky diodes is developed.
- Applications include WSNs, IoT, smart city infrastructures, wearable technology, biomedical implants, and emergency power systems.

The structure of this paper is as follows: Section II presents the design methodology, outlining the optimization approach using the proposed BGA. Section III details the rectenna optimization process using the BGA technique. Section IV analyses the rectenna's performance based on key metrics. Section V evaluates the design and performance of the dual-band rectifier. Section VI provides a comparative analysis of the proposed system against existing RF energy harvesting solutions. Section VII concludes the paper by summarizing key findings and discussing future research directions for AI-driven rectenna designs.

## **II. Design Methodology**

In rectenna topology optimization, the design area is divided into identical pixel blocks, each assigned as either air or conductor based on a binary mapping scheme. This transformation converts the design problem into a binary optimization challenge, where the goal is to determine the optimal rectenna structure for improved performance.

Traditional optimization methods often rely on iterative tuning and extensive simulations, which can be computationally expensive and time-consuming. To address these limitations, a Binary Genetic Algorithm (BGA), a class of evolutionary techniques inspired by natural selection—is employed to automate and enhance the design process. BGA is particularly advantageous in rectenna optimization, as it efficiently explores large solution spaces and identifies high-performing designs without exhaustive manual tuning.

Unlike conventional techniques, the genetic algorithm (GA) employs adaptive evolution, ensuring progressive improvement of the design over successive generations. In this study, the BGA offers several benefits:

- It systematically searches for optimal rectenna topologies by evaluating thousands of potential configurations, significantly reducing the need for manual intervention.
- Through selection, crossover, and mutation, it rapidly identifies high-performance designs avoiding the slow, trial-and-error approach of traditional methods.

- Repeated refinement ensures minimal reflection coefficient ( $S_{11}$ ) and maximized bandwidth, leading to a highly efficient rectenna design.
- Unlike gradient-based optimization methods, the GA's stochastic nature helps prevent premature convergence, reducing the risk of getting trapped in local optima.
- It can simultaneously optimize multiple performance parameters, such as gain, bandwidth, and radiation efficiency.

The GA-based optimization process involves several key steps:

1. *Initialization*: The genetic algorithm encodes the design parameters as genes, forming an initial population of chromosomes (i.e., rectenna design candidates). The typical population size ranges from 30 to 100 to balance computational efficiency and performance [17].
2. *Selection*: Chromosomes are ranked according to their fitness values, which are determined by performance metrics such as reflection coefficient and impedance bandwidth. Selection is performed either probabilistically or based on fitness scores, allowing the best candidates to advance to the next generation.
3. *Crossover*: Selected parent chromosomes are recombined to generate new gene sequences. This crossover operation creates offspring by blending genetic traits from both parents.
4. *Mutation*: To maintain genetic diversity and avoid premature convergence, small random variations are introduced into the gene pool. The mutation rate typically falls between 0.01 and 0.3 to ensure balanced exploration of the design space.
5. *Next Generation Formation*: A new population is formed by combining parents and offspring, effectively doubling the original size. The best-performing individuals are retained, while the least fit chromosomes are discarded.
6. *Convergence Check*: The algorithm evaluates whether the best fitness value meets a predefined threshold. If the criterion is satisfied, the process terminates. Otherwise, the algorithm iterates from Step 3 until convergence is achieved.

In optimizing the rectenna for RF energy harvesting, several design parameters must be finely tuned to ensure optimal performance. The BGA approach is applied to optimize the rectenna topology using an evolutionary process inspired by natural selection.

The key rectenna design parameters considered in the BGA include patch dimensions, slot geometry, feed line width, substrate thickness, and dielectric constant. These parameters directly impact impedance matching, bandwidth, gain, and radiation efficiency.

The objective (fitness) function used in the optimization process incorporates not only the reflection coefficient but also bandwidth, gain, radiation efficiency, and surface current distribution, enabling a comprehensive evaluation of performance. The fitness function is expressed as:

$$F = w_1 \times (|S_{11}|) + w_2 \times BW + w_3 \times G + w_4 \times \eta \quad (1)$$

where  $w_1$ ,  $w_2$ ,  $w_3$ , and  $w_4$  are weighting factors for each performance metric,  $BW$  is the bandwidth,  $G$  is the gain and  $\eta$  is the radiation efficiency of the rectenna. In our case, the considered target and weight are:

- Reflection coefficient ( $S_{11}$ ): Target = -15 dB; weight ( $w_1$ ) = 1. This weight is selected to minimize power reflection and maximize power transfer.

- Gain ( $G$ ): Target = 5 dBi at 2.45 GHz and 5.8 GHz; weight ( $w_2$ ) = 1. This weight is assigned equal importance to  $S_{11}$  since it directly impacts energy harvesting capability.
- Bandwidth ( $BW$ ): Target = 100 MHz; weight ( $w_3$ ) = 0.5. This weight is included for system stability, but it is less critical for energy harvesting applications.
- Efficiency ( $\eta$ ): Target = 90%; weight ( $w_4$ ) = 0.8. This weight is given high priority, but since efficiency is largely influenced by  $S_{11}$  and gain, it's assigned a slightly lower weight.

The BGA algorithm iteratively refines the rectenna geometry to maximize efficiency while minimizing computational overhead. The step-by-step workflow of the GA-based rectenna optimization process used in this study is illustrated in Fig. 1, while the optimized BGA parameters are listed in Table 2.

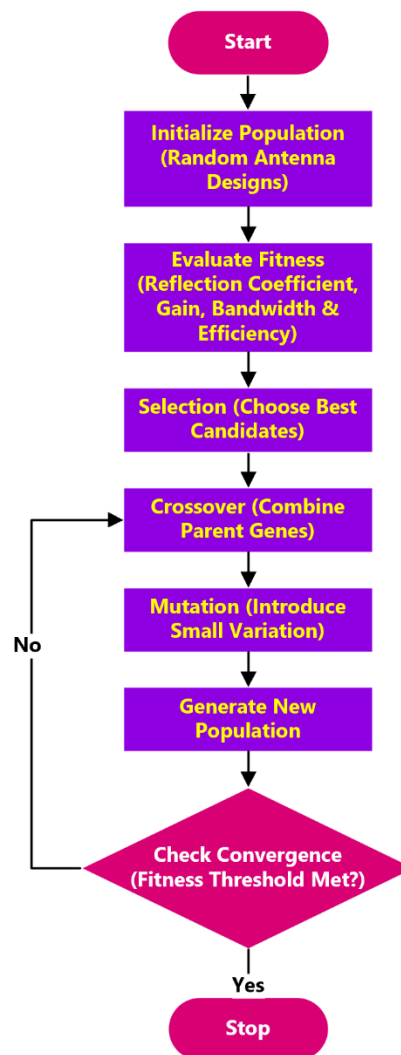


Fig. 1. Flowchart of BGA optimization process.

The convergence rate of the GA optimization follows a three-phase pattern:

1. Rapid improvement in early generations (1-50) as weak designs are eliminated.
2. Fine-tuning in the middle generations (50-150) to optimize bandwidth and efficiency.

3. Stabilization in the final generations (150-250), ensuring convergence within 20 stagnant iterations.

The GA process iterates continuously, optimizing the Microstrip Rectenna (MSA) geometry to maximize impedance bandwidth and enhance radiation characteristics. The optimized rectenna achieves an  $S_{11}$  of -40 dB, a 14% bandwidth improvement, and peak gains of 6.2 dBi (2.45 GHz) and 7.12 dBi (5.8 GHz).

Table 2: Binary Genetic Algorithm (BGA) parameters used in rectenna optimization.

Parameter	Value
Population Type	Bit String
Maximum Generations	250
Population Size	50
Selection Method	Roulette Selection
Crossover Rate	0.9
Crossover Type	Single Point Crossover
Mutation Rate	0.03
Iterations	50

### III. Rectenna Optimization Using BGA

The proposed rectenna design is based on a conventional aperture-coupled patch configuration. Initially, its geometrical parameters are calculated using standard microstrip design equations. However, to meet specific bandwidth and gain requirements, a full-wave electromagnetic analysis is necessary. To address this, a binary coding scheme is employed, simplifying the optimization process and easing fabrication of the stacked rectenna structure.

The overall structure of the microstrip rectenna, incorporating a strip-slot hybrid configuration with multiple layers, is shown in Fig. 2. The rectenna consists of two substrate layers separated by an air gap. The substrate material has a dielectric constant of 4.3 and a loss tangent of 0.02. The upper substrate hosts the radiating patches for 2.45 GHz and 5.8 GHz, while the lower layer contains a ground plane with a coupling aperture and a feeding microstrip line on its bottom side.

A horizontal slot on the top surface of the bottom layer (Fig. 2(c)) plays a crucial role in enhancing rectenna performance. It improves electromagnetic coupling between the feedline and radiating patch, enhancing power transfer efficiency and minimizing signal losses. The slot also acts as an impedance matching element, helping to reduce reflection coefficients and expand bandwidth. By carefully tuning its dimensions and placement, the rectenna maintains low reflection and efficient energy transfer.

Beyond matching, the slot influences surface current distribution and the excitation of radiation modes. This improves the directivity of the radiation pattern and reduces unwanted radiation effects. As a resonant element, the slot also enhances frequency selectivity, enabling efficient operation at both 2.45 GHz and 5.8 GHz.

The radiating patch was optimized using Ansoft HFSS (High-Frequency Structure Simulator), a widely used full-wave simulation tool for RF and microwave design. The BGA was integrated into HFSS through scripting to iteratively refine the patch geometry, with a fitness function based primarily on minimizing the reflection coefficient.

To enhance impedance bandwidth and radiation efficiency, the patch surface is divided into discrete unit cells, each represented by a binary code '1' for conductor and '0' for air. The BGA's evolutionary process includes three main operations: selection of high-fitness parent chromosomes, crossover to generate new designs, and mutation

to introduce variation and prevent premature convergence. This enables the discovery of efficient designs without manual tuning.

The initial design targets the 2.45 GHz band and is implemented on an FR-4 substrate (1.5 mm thickness). The patch is discretized into 160 unit cells arranged in a  $10 \times 16$  grid, each measuring  $1.95 \times 1.95 \text{ mm}^2$ . Each unit is treated as a gene encoded with a binary value: '1' for a metal pixel (yellow), and '0' for air (green). Overlaps between adjacent cells are adjusted to maintain electrical continuity, with the structure represented by a binary matrix.

The patch geometry is encoded as a binary string, where each unique string corresponds to a distinct rectenna design. Optimization is performed by modifying the binary string values iteratively. To prevent disconnected conductor regions, isolated '0' cells surrounded by '1's are converted to '1', and vice versa. This approach ensures both structural and electrical integrity while maintaining compact physical dimensions.

A fitness function is used to evaluate rectenna performance, prioritizing reflection coefficient minimization and bandwidth maximization. The fitness function is calculated based on the  $S_{11}$  parameter, where:

- If  $S_{11} < -15 \text{ dB}$ , the fitness function is set to 0, indicating an optimal match.
- If  $S_{11} \geq -15 \text{ dB}$ , the bandwidth is further assessed as part of the optimization criteria.

By continuously refining the binary string representation, the GA process identifies an optimized patch design that meets the target impedance matching and bandwidth requirements.

$$\text{fitness}(F) = \frac{1}{N} \sum_{i=1}^N S_{11} \quad (2)$$

$$\text{where } S_{11}(\text{dB}) = \begin{cases} S_{11}(\text{dB}) + 15 \text{ dB}, & S_{11}(\text{dB}) \geq -15 \text{ dB} \\ 0, & S_{11}(\text{dB}) < -15 \text{ dB} \end{cases} \quad (3)$$

$N$  represents the number of sampling frequencies within the specified frequency band. The reflection coefficient should be minimized at the resonance frequency to ensure optimal impedance matching.

The proposed Binary Genetic Algorithm (BGA) is employed as an electromagnetic optimization technique in conjunction with Ansoft HFSS. The optimization is carried out using HFSS scripting, with the parameters summarized in Table 3. The GA runs iteratively until the fitness function either reaches a predefined threshold or remains unchanged for 20 consecutive generations, signalling convergence.

Table 3. HFSS-integrated BGA simulation settings for rectenna optimization.

Population type	Bit String
Maximum number of generations	250
Population size	50
Selection	Roulette
Crossover rate	0.9
Crossover	Single point crossover
Mutation rate	0.03
Iterations	50

In this process, the binary-coded GA optimizes the patch geometry by adjusting the first 120 genes of each chromosome, resulting in a vast solution space of  $2^{160}$

possible configurations. Compared to traditional full-wave analysis methods, which demand substantial computational resources and time, the BGA significantly accelerates the optimization, achieving high-performance designs within a few hours.

The optimized patch for 2.45 GHz achieves a reflection coefficient below -40 dB, indicating excellent impedance matching. The final structure is shown in Fig. 2(a), and detailed rectenna dimensions are listed in Table 4.

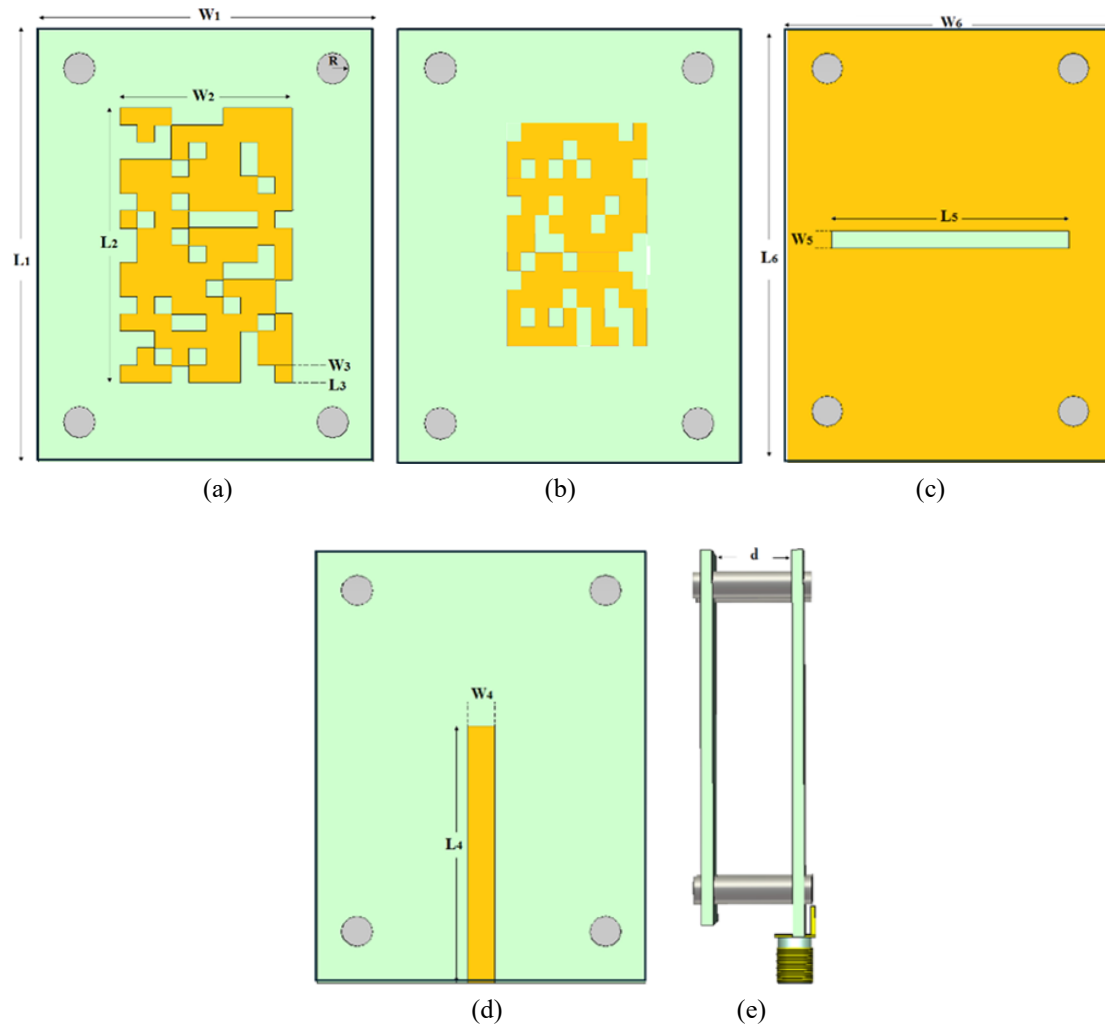


Fig. 2. Configuration of the proposed rectenna: (a) Top patch of the first layer, (b) Bottom patch of first layer, (c) Top view of the second layer, (d) Bottom view of the second layer, and (e) 3D view.

A second round of BGA simulations was conducted to optimize the patch geometry for 5.8 GHz operation. Here, the patch area was discretized into 120 unit cells arranged in a  $10 \times 12$  grid. The rectenna was designed on a substrate with a thickness of 0.8 mm, where each unit cell measured  $1.2 \times 1.2 \text{ mm}^2$ . Each cell, treated as a gene, was assigned a binary value: '1' representing a metal pixel (orange) and '0' representing air (white).

Simulation results show that the 5.8 GHz design achieves a bandwidth ( $S_{11} \leq -10 \text{ dB}$ ) from 5.16 GHz to 5.2 GHz, with a resonant frequency centred at 5.5 GHz. The corresponding physical dimensions are provided in the final column of Table 4.

Table 4. Physical dimensions of the optimized rectenna structure.

Parameters	Top patch (mm)	Bottom patch (mm)
$W_1$	34	17
$L_1$	45	22
$W_2$	19	13
$L_2$	28	14
$W_3$	1.9	1.2
$L_3$	1.9	1.2
$W_4$	3.2	1.3
$L_4$	29	13
$W_5$	2.1	1
$L_5$	25	12
$W_6$	35	21
$L_6$	45	23
R	1.7	1.7
D	11	5.7
H	1.2	0.8

#### IV. Rectenna Performance Analysis

The performance of the optimized rectenna was evaluated based on its reflection coefficient, radiation pattern, and gain. Simulations were conducted using HFSS, and to experimentally validate the results, two prototypes were fabricated, as shown in Fig. 3. The reflection coefficient of the fabricated rectenna was measured using a LibreVNA, an open-source, USB-based vector network analyzer with two ports.

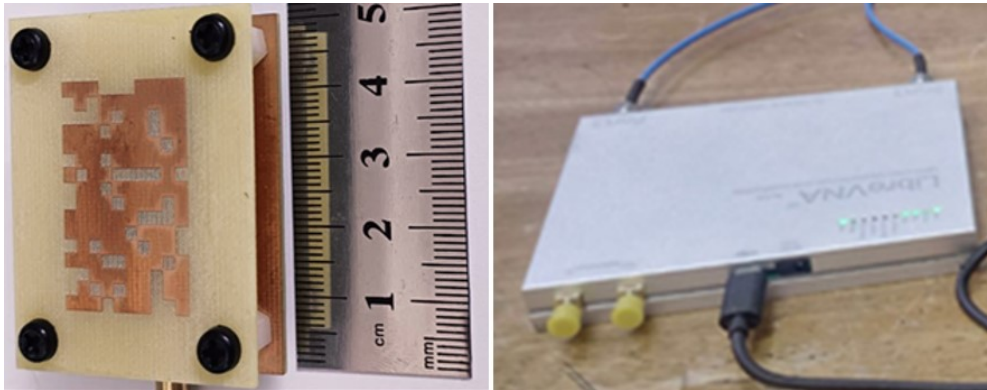


Fig. 3. Fabricated rectenna prototype.

The measured and simulated  $S_{11}$  spectra are presented in Fig. 4(a). The simulated results indicate a bandwidth ranging from 2.35 GHz to 2.54 GHz, with a minimum  $S_{11}$  value of -41 dB at the resonant frequency. The measured bandwidth extends slightly further, from 2.38 GHz to 2.58 GHz, showing strong agreement with the simulation. Minor discrepancies can be attributed to fabrication imperfections and environmental influences, such as free-space measurement conditions.

At 5.8 GHz, the simulation predicts a broad bandwidth from 5.16 GHz to 6 GHz, while the measured bandwidth is slightly narrower, about 150 MHz, spanning 5.14 GHz to 5.95 GHz. These deviations are likely due to factors such as imprecise substrate thickness and minor errors introduced during the soldering process.

Fig. 4(b) compares the simulated and measured gain spectra across the frequency range. The rectenna achieves peak gains of 7 dBi at 2.45 GHz and 7.5 dBi at 5.8 GHz, validating the effectiveness of the optimization approach.

Fig. 4(c) presents the radiation patterns at 2.45 GHz, showing good agreement between simulation and measurement. The radiation patterns at 5.8 GHz in both the E-plane and H-plane are shown in Fig. 4(d), confirming the rectenna's dual-band directive behaviour.

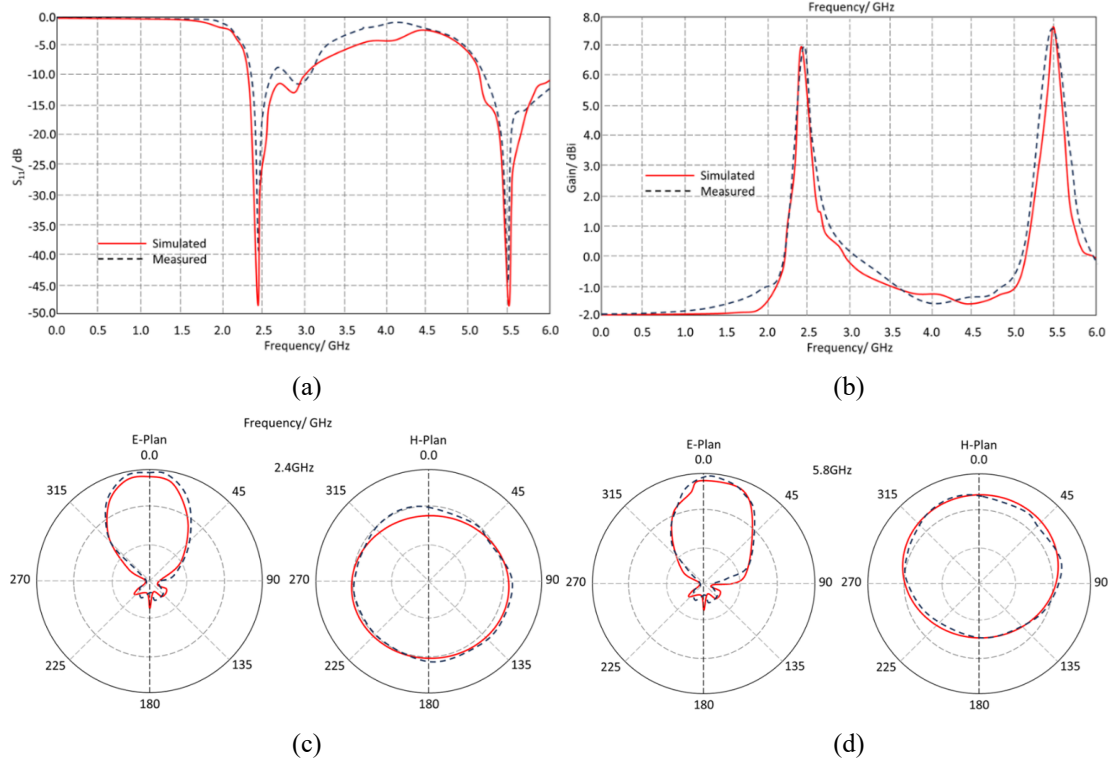


Fig. 4. Simulated and measured performance of the proposed dual-band rectenna. (a) Reflection coefficient ( $S_{11}$ ) spectra at 2.45 GHz and 5.8 GHz showing excellent impedance matching. (b) Gain spectra highlighting peak gains of 7 dBi at 2.45 GHz and 7.5 dBi at 5.8 GHz. (c) Radiation patterns at 2.45 GHz in the E-plane and H-plane from both simulation and measurement. (d) Radiation patterns at 5.8 GHz in the E-plane and H-plane, demonstrating directive behavior and dual-band operation.

## V. Dual-Band Rectifier Design and Evaluation

The commercial rectifier board was originally designed to operate across six frequency bands for RF energy harvesting. In this study, we focused on optimizing its performance specifically at 2.45 GHz and 5.8 GHz, as illustrated in Fig. 5.

To meet the requirements for high power-handling capability, low input voltage, and enhanced DC output, a voltage doubler topology was employed. The rectifier is based on the Powercast Corporation P21XXCSR-EVB board (see Fig. 5) and uses Skyworks SMS7630 and Avago HSMS-285B Schottky diodes, chosen for their low threshold voltage and high sensitivity at low input power—ideal characteristics for RF energy harvesting applications.

The rectifier's impedance matching is influenced by several factors, including operating frequency, input power level, and the load resistor-inductor network. To ensure efficient energy conversion, these parameters were carefully optimized. A 1 k $\Omega$  load resistance was used, and matching was achieved through a combination of single-stub tuning, a radial stub, a meander-line taper, and an inter-digital capacitor. Additionally, a 68 pF capacitor was implemented as a low-pass filter, allowing only the DC component to reach the load.

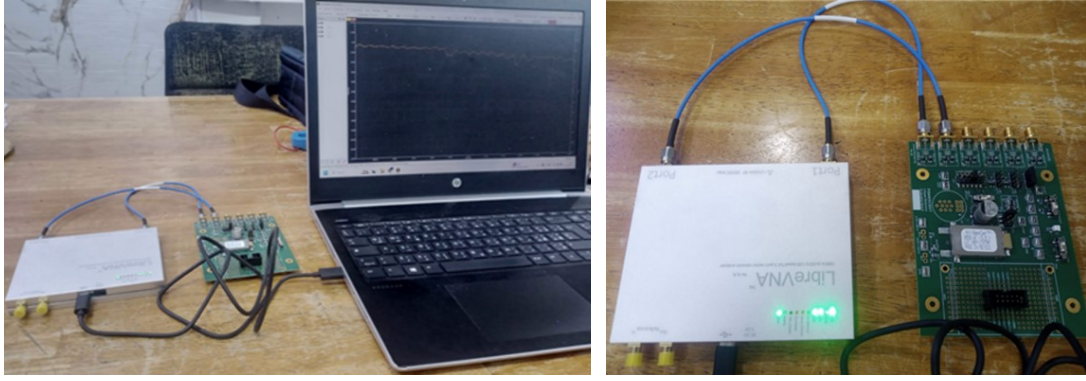


Fig. 5: Commercial rectifier module used for dual-band RF energy harvesting. Photograph of the Powercast P21XXCSR-EVB board under test, configured for 2.45 GHz and 5.8 GHz operation. The circuit integrates a voltage doubler topology with Skyworks SMS7630 and Avago HSMS-285B Schottky diodes, optimized using stub tuning, radial stub, meander-line taper, and inter-digital capacitor. A 68 pF capacitor is used as a low-pass filter to extract the DC output.

The  $S_{11}$  spectra of the proposed RF harvester were measured to confirm resonance at the target frequency bands, as shown in Fig. 6. The measured  $S_{11}$  results closely align with the simulated response at both 2.45 GHz and 5.8 GHz, exhibiting only minor deviations in magnitude. The rectifier circuit demonstrates effective impedance matching, maintaining  $S_{11}$  values below  $-10$  dB across 2.2–3.3 GHz and 5.3–6 GHz, thereby covering the desired frequency bands for efficient RF energy harvesting.

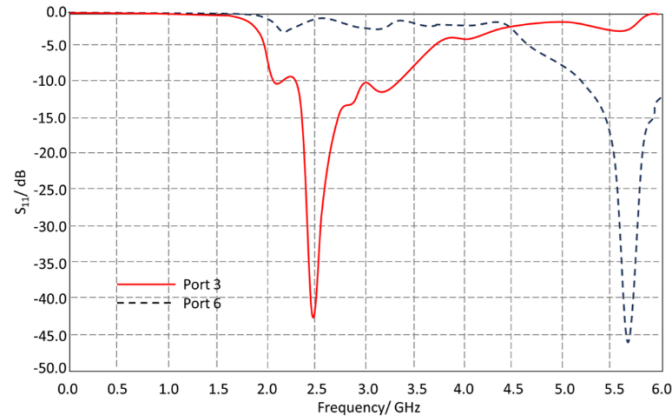


Fig. 6. Measured reflection coefficient ( $S_{11}$ ) of the RF harvester at 2.45 GHz and 5.8 GHz. The rectifier demonstrates effective impedance matching, with  $S_{11}$  values below  $-10$  dB across the desired bands. The measured resonance closely aligns with simulated results, indicating robust dual-band tuning.

A deeper understanding of the dual-band rectifier's performance is obtained through parametric study. The RF-to-DC conversion efficiency ( $\eta_{RF-DC}$ ) depends on the available input RF power. Figure 7 shows both measured and simulated values of  $\eta_{RF-DC}$  at 2.45 GHz and 5.8 GHz as functions of input power. Peak efficiencies of 90% at 2.45 GHz and 52% at 5.8 GHz are achieved at an input power of 6 dBm. At a lower input power of 0 dBm, the rectifier maintains efficiencies of 57% and 30% at 2.45 GHz and 5.8 GHz, respectively.

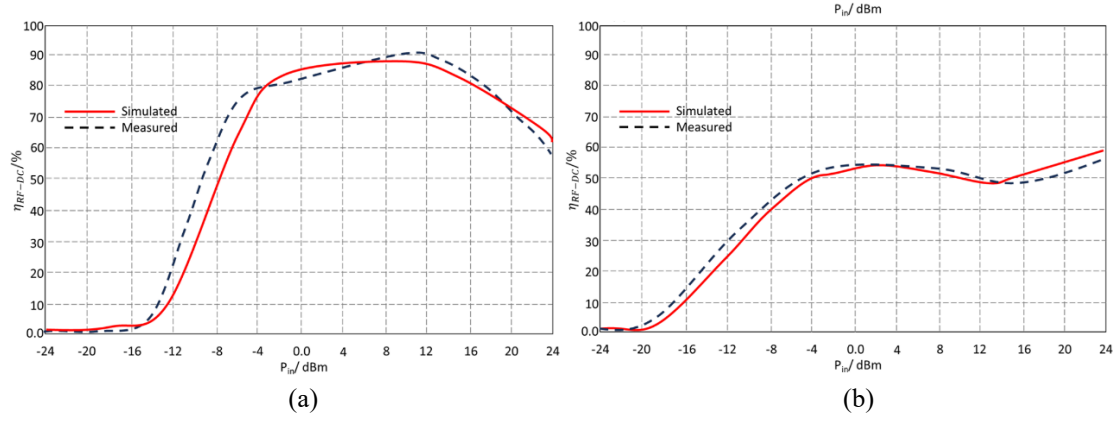


Fig. 7. Measured and simulated RF-to-DC conversion efficiency versus input power. (a) Conversion efficiency at 2.45 GHz; peak efficiency of 90% achieved at 6 dBm. (b) Conversion efficiency at 5.8 GHz; peak efficiency of 52% achieved at 6 dBm. The rectifier maintains high efficiency even at low input power levels, confirming its suitability for ambient RF harvesting.

Figure 8 presents the RF-to-DC conversion efficiency as a function of input power for various load resistances. The results clearly indicate that efficiency decreases as the load resistance increases. The highest efficiency is consistently achieved with a 1 k $\Omega$  load across all tested power levels. For example, at 5.8 GHz and an input power of 5 dBm, the rectifier reaches approximately 50% efficiency with a 1 k $\Omega$  load. In contrast, under the same conditions, the efficiency drops to around 8–10% when the load resistance is increased to 5 k $\Omega$ .

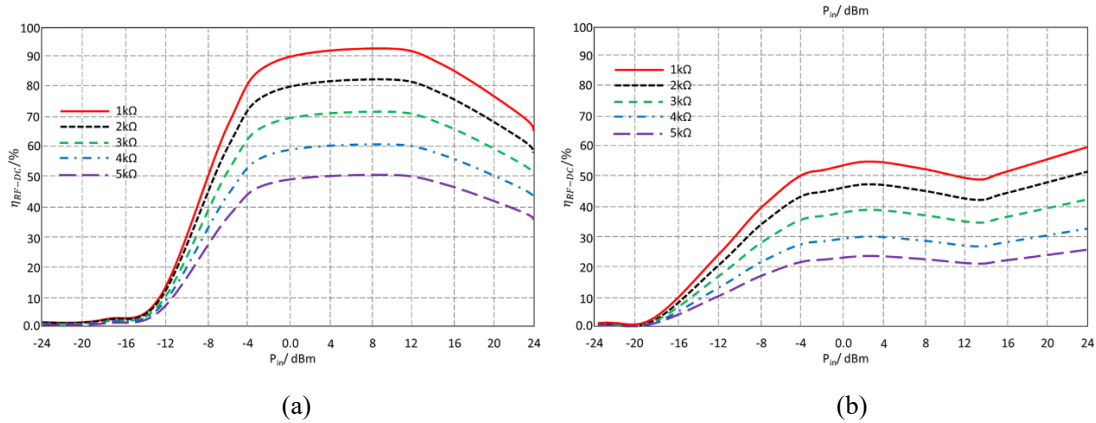


Fig. 8. Simulated conversion efficiency versus input power for various load resistances. (a) At 2.45 GHz, and (b) At 5.8 GHz. Efficiency decreases as load resistance increases, with optimal performance consistently observed at a 1 k $\Omega$  load.

The experimental setup for measuring the output DC voltage of the dual-band rectifier employs an Agilent N5183 RF signal generator, capable of operating up to 20 GHz. The generator is configured to sweep the input power ( $P_{in}$ ) from  $-24$  dBm to 24 dBm. The output DC voltage is then recorded as a function of input power at the corresponding frequencies.

Figure 9 shows both measured and simulated output DC voltages at 2.45 GHz and 5.8 GHz, respectively. At an input power of 0 dBm, the measured DC voltages are 1.9 V at 2.45 GHz and 1.2 V at 5.8 GHz. These results confirm the effective performance of the dual-band rectifier and demonstrate that pairing it with the proposed rectenna significantly enhances the output voltage for RF energy harvesting applications.

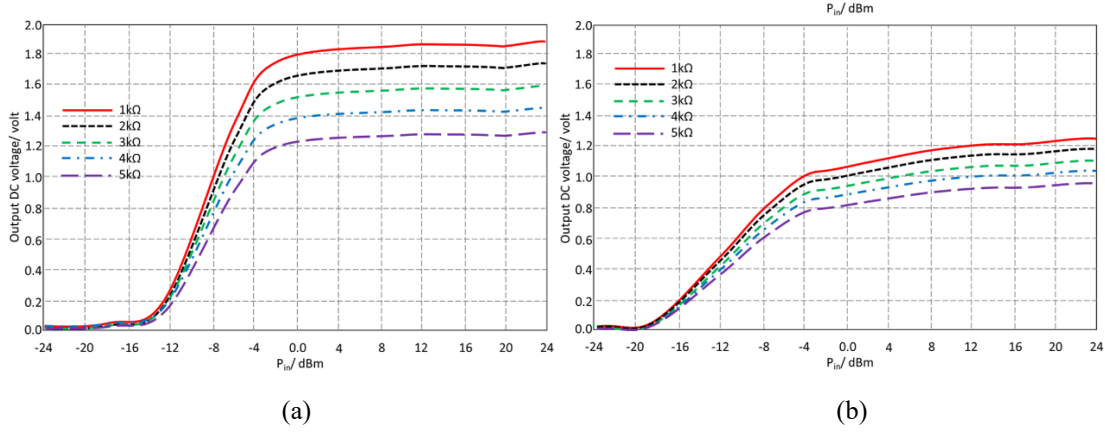


Fig. 9. Measured output DC voltage as a function of input RF power across various load conditions. (a) At 2.45 GHz, and (b) At 5.8 GHz. The rectifier delivers a DC voltage of 1.9 V at 2.45 GHz and 1.2 V at 5.8 GHz under 0 dBm input power, validating its effective dual-band energy harvesting performance.

## VI. Comparison with Existing RF Energy Harvesting Systems

Table 6 provides a comparative analysis between the proposed RF energy harvesting system and existing works in the literature. Key distinguishing features of the proposed system include:

- *Frequency Range*: The system operates at 2.45 GHz and 5.8 GHz, aligning with common standards while offering broader coverage than many existing designs.
- *Peak Efficiency*: It achieves a peak RF-to-DC conversion efficiency of 90% at 11 dBm for 2.45 GHz—substantially higher than most reported systems. For comparison, the next highest efficiency in the literature is 63%, as noted in [18] and [19].
- *Ambient Source Utilization*: Unlike many prior designs that rely on a single-band or narrowband source, this system leverages multiple ambient RF bands, significantly improving overall energy collection.
- *Design and Optimization*: The rectenna structure is implemented on an FR-4 substrate and optimized using a Binary Genetic Algorithm (BGA) to ensure efficient dual-band operation at the desired resonances and gains.

Overall, the proposed system stands out due to its high efficiency, dual-frequency harvesting capability, and AI-driven design optimization. The integration of BGA enhances performance and scalability, positioning the system as a notable advancement over prior designs. These innovations make it a promising candidate for IoT applications, wireless sensor networks (WSNs), and energy-autonomous devices in next-generation 5G and sub-6 GHz environments.

Table 6. Comparison of the proposed RF energy harvesting system with existing designs.

Ref.	Freq. (GHz)	Peak $\eta$ (%) @ $P_{in}$ (dBm)	Ambient source	Substrate	Diode
[18]	1.8	63 @0	Yes	R04003 & R05870	SMS7630
[19]	0.9	63 @0	No	FR4	HSMS285C
[20]	1.8/2.5	24 @-20	Yes	FR4	HSMS2850
[21]	1.8/2.5	24 @-20	Yes	FR4	HSMS2850
[22]	0.3-16	30 @0	No	FR 4	HSMS 2820
[23]	2.4/5.8	30 @14	No	FR 4	HMPS2822

[24]	1.8	51 @-10	Yes	RO4003 R05880	HSMS2850
[25]	2.5/3.6	59.4 @2	No	R04003	SMS7630
[26]	1.82/2.1/2.4/2.66	31.7/23.5/25.4/15.5 @-20	Yes	R05880	HSMS2850
[27]	0.92/1.82/2.1/2.46/2.65	31.8/24/22.7/15/14.1 @-20	Yes	RT/Duroid 5880	HSMS2850
This work	2.45/5.8	90 @11	Yes	FR-4	HSMS2860

## VII. Conclusion

This paper presents a compact, dual-band RF energy harvesting system optimized using a Binary Genetic Algorithm (BGA). The proposed rectenna design achieves excellent impedance matching and high gain at 2.45 GHz and 5.8 GHz, validated through both simulation and measurement. A commercial rectifier module incorporating a voltage doubler topology and Schottky diodes (SMS7630 and HSMS-285B) was customized and tuned for the target frequency bands, delivering peak RF-to-DC conversion efficiencies of 90% and 52%, respectively.

At low input power levels (0 dBm), the system maintains high conversion efficiency, demonstrating strong adaptability to real-world ambient RF environments. Furthermore, outdoor testing confirms stable DC output voltages, supporting the rectifier's effectiveness under practical conditions.

The combination of AI-driven optimization and robust hardware implementation makes the proposed system highly suitable for energy-autonomous applications such as wireless sensor networks, IoT devices, smart city infrastructure, and biomedical implants. The rectenna's ability to operate efficiently across variable environmental conditions and its compatibility with sub-6 GHz 5G bands position it as a strong candidate for next-generation sustainable wireless systems.

**Acknowledgment:** Princess Nourah bint Abdulrahman University Researchers Supporting Project number (PNURSP2025R828), Princess Nourah bint Abdulrahman University, Riyadh, Saudi Arabia.

## Open Research

**Availability Statement:** No new data was created for this study.

## References

- [1] Hsu, C.Y.; Lin, S.C.; Tsai, Z.M. Quadband rectifier using resonant matching networks for enhanced harvesting capability. *IEEE Microw. Wirel. Components Lett.* 2017, 27, 669–671.
- [2] Shen, S.; Chiu, C.Y.; Murch, R.D. A dual-port triple-band L-probe microstrip patch rectenna for ambient RF energy harvesting. *IEEE Antennas Wirel. Propag. Lett.* 2017, 16, 3071–3074.
- [3] Chandravanshi, S.; Sarma, S.S.; Akhtar, M.J. Design of triple band differential rectenna for RF energy harvesting. *IEEE Trans. Antennas Propag.* 2018, 66, 2716–2726.
- [4] Liu, J.; Zhang, X.Y. Compact triple-band rectifier for ambient RF energy harvesting application. *IEEE Access* 2018, 6, 19018–19024.
- [5] Shen, S.; Zhang, Y.; Chiu, C.Y.; Murch, R.D. A triple-band high-gain multibeam ambient rf energy harvesting system utilizing hybrid combining. *IEEE Trans. Ind. Electron.* 2019, 67, 9215–9226.

- [6] Tafekirt, H.; Pelegri-Sebastia, J.; Bouajaj, A.; Reda, B.M. A sensitive triple-band rectifier for energy harvesting applications. *IEEE Access* 2020, 8, 73659–73664.
- [7] Mohammed A. Al-Mihrab; Ali J. Salim; Jawad K. A. A Compact multiband printed monopole antenna with hybrid polarization radiation for GPS, LTE, and satellite applications. *IEEE Access* 2020, 110371-110380.
- [8] Roy, S., et al. Quad-band multiport rectenna for RF energy harvesting in ambient environment. *IEEE Access*, 2021, vol.9, 77464-77481.
- [9] Muncuk, U.; Alemdar, K.; Sarode, J.D.; Chowdhury, K.R. Multiband ambient RF energy harvesting circuit design for enabling batteryless sensors and IoT. *IEEE Internet Things J.* 2018, 5, 2700–2714.
- [10] Liu, Z.; Ma, S.; and Zhang, X. Optimization of rectenna design using genetic algorithm for efficient energy harvesting. *IEEE Transactions on Antennas and Propagation*, 2020, 68(4), 2874-2882.
- [11] Bairappaka, S.K.; et al. Novel design of broadband circularly polarized rectenna with enhanced gain for energy harvesting. *IEEE Access*, 2024, 12, 65583-65594.
- [12] Ha, T.D.; et al. A Low-Profile, Wide-angle, and bandwidth-enhanced rectenna for radiative energy harvesting in the 12 GHz band. *IEEE Microwave and Wireless Technology Letters*, 2024, 23(11), 3807-3811.
- [13] Han, Y.; Kim, E.; Lee, A.H.L. Flat-panel-rectenna with broad RF energy harvesting coverage for wireless-powered sensor applications. *IEEE Access*, 2024, 13, 6146-6153.
- [14] Abushab, M.; et al.; Hybrid Energy Harvester Based on Bowtie Periodic Antenna Surface. *IEEE Access*, 2025, 13, 14417-14425.
- [15] Kumar, S.; et al. A compact stacked multisector near-isotropic coverage rectenna array system for IoT applications. *IEEE Microwave and Wireless Technology Letters*, 2024, 34(1), 123-126.
- [16] Zhang, Y., Wang, J., and Chen, L. Machine learning-based design optimization for high-efficiency rectennas. *Journal of Applied Physics*, 2021, 129(15),154901.
- [17] Deb, K. (2001). *Multi-Objective Optimization Using Evolutionary Algorithms*. John Wiley and Sons.
- [18] Singh, M.; Agrawal, S.; Parihar, M.S. Design of a rectenna system for GSM-900 band using novel broadside 2×1 array antenna. *J. Eng.* 2017, 2017, 232–236.
- [19] Agrawal, S.; Parihar, M.S.; Kondekar, P.N. A dual-band rectenna using broadband DRA loaded with slot. *Int. J. Microw. Wirel. Technol.* 2018, 10, 59.
- [20] Adam, I.; M. Yasin, M.N.; A. Rahim, H.; Soh, P.J.; Abdulmalek, M.F. A compact dual-band rectenna for ambient RF energy harvesting. *Microw. Opt. Technol. Lett.* 2018, 60, 2740–2748.
- [21] Alex-Amor, A.; Palomares-Caballero, Á.; Fernández-González, J.M.; Padilla, P.; Marcos, D.; Sierra-Castañer, M.; Esteban, J. RF energy harvesting system based on an archimedean spiral antenna for low-power sensor applications. *Sensors* 2019, 19, 1318
- [22] Bhatt, K.; Kumar, S.; Kumar, P.; Tripathi, C.C. Highly efficient 2.4 and 5.8 GHz dual-band rectenna for energy harvesting applications. *IEEE Antennas Wirel. Propag. Lett.* 2019, 18, 2637–2641.

- [23] Partal, H.P.; Belen, M.A.; Partal, S.Z. Design and realization of an ultra-low power sensing RF energy harvesting module with its RF and DC sub-components. *Int. J. RF Microw. Comput.-Aided Eng.* 2019, 29, e21622.
- [24] Shen, S.; Zhang, Y.; Chiu, C.Y.; Murch, R. Directional multiport ambient RF energy harvesting system for the internet of things. *IEEE Internet Things J.* 2020, 8, 5850–5865.
- [25] Chandrasekaran, K.T.; Agarwal, K.; Nasimuddin; Alphones, A.; Mitra, R.; Karim, M.F.; Compact dual-band metamaterial-based high-efficiency rectenna: an application for ambient electromagnetic energy harvesting. *IEEE Antennas Propag. Mag.* 2020, 62, 18–29.
- [26] Muhammad, S.; Tiang, J.J.; et al.; Efficient quad-band RF energy harvesting rectifier for wireless power communications. *AEU – Int. Journal of Electronics and Communications*, Volume 139, September 2021, 153927.
- [27] Surajo Muhammad, Jun Jiat Tiang, Sew Kin Wong, Amjad Iqbal, Amor Smida, Mohamed Karim Azizi, "A Compact Dual-Port Multi-Band Rectifier Circuit for RF Energy Harvesting", *Computers, Materials & Continua* 2021, 68(1), 167-184.